

Detection of onset of failure in prestressed strands by cluster analysis of acoustic emissions

Marianna Ercolino^{1a}, Alireza Farhidzadeh^{2b}, Salvatore Salamone^{*3} and Gennaro Magliulo^{1c}

¹Department of Structures for Engineering and Architecture, University of Naples Federico II, Via Claudio 21, 80125 Naples, Italy

²Mistras Group Inc., 195 Clarksville Rd, Princeton Junction, NJ 08550, USA

³Department of Civil, Architectural and Environmental Engineering, University of Texas at Austin, 301 E Dean Keeton, C1748, Austin, TX, 78712, USA

(Received November 26, 2014, Revised July 10, 2015, Accepted July 25, 2015)

Abstract. Corrosion of prestressed concrete structures is one of the main challenges that engineers face today. In response to this national need, this paper presents the results of a long-term project that aims at developing a structural health monitoring (SHM) technology for the nondestructive evaluation of prestressed structures. In this paper, the use of permanently installed low profile piezoelectric transducers (PZT) is proposed in order to record the acoustic emissions (AE) along the length of the strand. The results of an accelerated corrosion test are presented and k-means clustering is applied via principal component analysis (PCA) of AE features to provide an accurate diagnosis of the strand health. The proposed approach shows good correlation between acoustic emissions features and strand failure. Moreover, a clustering technique for the identification of false alarms is proposed.

Keywords: corrosion; acoustic emission; principal component analysis; k-means method

1. Introduction

Prestressed concrete (PC) is widely used for applications ranging from commercial buildings and bridges, to pressure vessels, tanks and containment vessels for nuclear power plants. Due to the increasing use of PC and the large number of PC structures in the US inventory, the corrosion of the steel strands is a concern for designers, owners and regulators. Indeed, the integrity of these structures could be seriously compromised by the strand failure due to corrosion (Naito *et al.* 2010). Extensive inspection and maintenance/repair programs have been established in the last few years, with attendant direct manpower, materials costs and significant indirect costs due to traffic and related business interruption.

Evaluation of strands in PC structures is challenging. Their general inaccessibility makes

*Corresponding author, Assistant Professor, E-mail: salamone@utexas.edu

^a Postdoctoral Fellow, E-mail: marianna.ercolino@unina.it

^b Ultrasonics Research Scientist, Email: alireza.farhidzadeh@gmail.com

^c Assistant Professor, E-mail: gmagliul@unina.it

evaluation difficult, costly and often inconclusive. Visual inspection is the simplest, oldest and most common form of evaluation. However there may be no outward signs that the strand has broken (Salamone *et al.* 2012). Several nondestructive evaluation (NDE) techniques for evaluating the condition of strands have been developed to address these issues in the past few years. Electrochemical methods, such as half-cell potential have been used to help understand the corrosion state within a concrete structure (ASTM 2009); however these methods can be highly affected by external conditions, leading to erroneous judgments (Li *et al.* 1998) and requiring long operations and deployment of specialized personnel (Mangual *et al.* 2013). In addition, they have been validated in reinforced concrete elements rather than for PC structures (Andrade *et al.* 2004, Choi *et al.* 2008, Elsener *et al.* 2003). Techniques based on guided ultrasonic waves (GUWs) have been used to monitor the evolution of the corrosion deterioration in reinforced mortar specimens (Ervin *et al.* 2009) as well as in post-tensioned systems.

The results presented in this paper are part of a long-term project that aims at developing a structural health monitoring (SHM) technology for the nondestructive evaluation of PC structures. Overall it is proposed to use permanently installed low profile piezoelectric transducers (PZT) to receive acoustic emissions (AE) along the length of the strand. A statistical approach based on Principal Component Analysis (PCA) and K-means clustering is proposed to detect the onset of failure of the strand during an accelerated corrosion test. Some considerations on the capability of the proposed approach are also reported in order to underline some possible future developments. The paper is organized as follows. A brief introduction to the AE technique and the proposed statistical approach (i.e., PCA and k-means) is given in the next section. Then, the experimental setup of the accelerated corrosion test is described, followed by the results. Finally conclusions are provided.

2. Background

2.1 Acoustic emission

The Acoustic Emission (AE) method is a nondestructive technique based on propagation of stress waves generated by sudden strain relief, such as cracking in structural materials. Acoustic emissions are elastic transient waves that can be detected by one or more piezoelectric sensors. The signals are preamplified, recorded, filtered, and representative features are extracted. Data analysis approaches are usually based on AE features and they are called parametric methods. In the following a brief summary of the main parameters of AE is reported.

The AE parameters can be divided in two categories: hit-driven and time-driven data. The hit-driven parameters are evaluated for each AE hit, i.e. for each signal voltage exceeding a pre-defined threshold (dash-dot line in Fig. 1). The most common features are illustrated in Fig. 1 and summarized in Table 1. On the contrary, the time-driven data are evaluated by recording the signal at a constant rate for intervals of pre-determined length, independent of any threshold setting (Table 1). These parameters are very useful since they represent a continuous AE signal, independent of threshold.

The AE method was first introduced in the early 90th as a monitoring technique for the corrosion detection in structural materials (Li *et al.* 1998, Mazille *et al.* 1995). Mazille *et al.* (1995) investigated the AE technique for the corrosion in austenitic steel, finding a good correlation between the AE activity (number of events) and the pitting corrosion damage. Moreover, the

authors presented the specific values of some main AE features, representing a first reference on the characteristics of these emissions. Li *et al.* (1998) reported the results of a systematic study on feasibility of AE in detecting rebar corrosion in either HCl solution or in concrete. Concerning the performed tests on single steel bars, all the experiments demonstrated that the AE activities have a high correlation with the corrosion process and rate in the rebar. According to these works on the corrosion of single steel reinforcing elements, AE is expected to be a plausible technique for corrosion damage detection. In the following years several studies were conducted to investigate this technique at the aim of evaluating the damage characteristics (Farhidzadeh *et al.* 2013b, Ohno and Ohtsu 2010) and the damage location (Niri *et al.* 2013).

Concerning PC elements, several studies were recently developed. Mangual *et al.* (2013) examined a series of PC elements under accelerated corrosion tests up to the pitting damage in the steel strands. The capability of AE in detecting the corrosion damage was demonstrated; however, the definition of the damage was highly dependent on other monitoring systems. In this work, the authors also proposed a method for the corrosion damage localization as a very interesting damage assessment tool that should be improved in order to evaluate its efficiency in terms of quantitative identification criteria. Elfergani *et al.* (2013) studied the Acoustic Emission (AE) technique in order to detect and locate the early stages of corrosion in PC elements. The authors demonstrated the capability of AEs in both identifying macro-cracks and crack propagation and classifying different crack types (i.e., shear and tensile cracks). Acoustic emission was also used to detect the onset of corrosion as well as the different levels of corrosion, as reported in ElBatanouny *et al.* (2014b).

In the past few years, the AE technique was investigated as a SHM system; however, unanswered questions have been posed regarding their reliability and accuracy. The inherent uncertainty in AE measurements, caused, for instance, by the presence of noise due to vibration, fretting, electromagnetic interference may hamper their reliability in terms of automatic damage detection. In many cases, traditional signal processing techniques, such as filtering and spectrum analysis, are insufficient to discriminate the events of interest, that is, those due to crack growth or imminent failure, from noise of various natures in a large dataset; therefore new alternatives have to be explored (Behnia *et al.* 2014). In many cases, hence, the noise is not identified by specific features values, such as a range of frequency, as it can happen in more common filters used in earthquake engineering applications (i.e., acceleration signals). Therefore, the definition of a unique and specific filtering criterion cannot be easily defined.

2.2 Principal component analysis

Principal Component Analysis (PCA) is a multivariate statistical procedure that transforms a set of correlated parameters in a set of new linearly uncorrelated variables, called principal components. The input vector \mathbf{X} is a p - n dimension vector, where n is the dimension of the observations (number of samples) and p the number of variables. By performing a linear transformation, a new k -dimensional vector \mathbf{Z} is defined as

$$PCA \begin{bmatrix} X_1 \\ \dots \\ X_n \end{bmatrix} \Rightarrow \begin{bmatrix} Z_1 \\ \dots \\ Z_n \end{bmatrix} \quad (1)$$

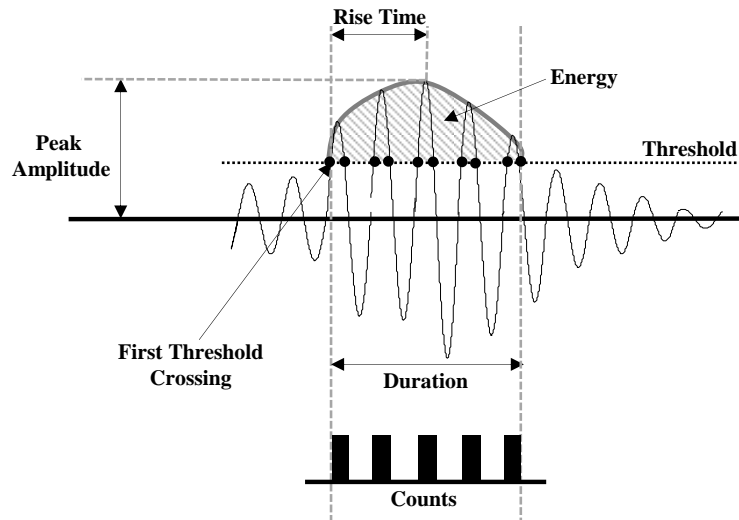


Fig. 1 Main features of the AE waveform

Table 1 Main features of the AE waveform (Physical Acoustics 2009)

Typology	Feature	Description
Hit-driven	Energy	Integral of the rectified voltage signal over the duration of the AE hit, e.g. the voltage-time units
	Average Frequency	Average frequency on the entire hit. It is evaluated as the ratio between the AE counts and the duration
	Signal Strength (SS)	Integral of the rectified voltage signal over the duration of the AE waveform
	RA	Ratio between rise time and peak amplitude
Time-driven	Absolute Energy (AbE)	True energy measure of the AE hit. It is derived as the integral of the squared voltage signal divided by the reference. resistance over the duration of the AE waveform packet
	RMS	Root Mean Square is a measure of the variation of the AE activity along the time. It is defined as the rectified, time averaged AE signal.
	ASL	Average Signal Level is a measure of the variation and averaged amplitude of the AE signal.

If $[x_{1j}, x_{2j}, x_{3j}, \dots, x_{pj}]$ is the input values of the j -th sample, the element z_{kj} is the k -th principal component at the j -th sample, evaluated as

$$z_{kj} = \sum_{h=1}^p \beta_{kh} \cdot x_{hj} \quad (2)$$

The coefficient β_{kh} in (2) are defined in such a way that the first combination (first principal component) has the maximum variance among the other infinite linear combination of the data set.

The number of principal components is equal to the number of original variables in the vector \mathbf{X} . However, the study of the first few components can take into account the most of variability in the data; as a consequence, it is possible to develop a deeper understanding of the investigated phenomenon by examining a reduced number of data; this procedure would not induce a reduction of the information from the raw data.

In this paper, the PCA was used to determine correlation interdependencies between AE features and corrosion damage in the steel strand. PCA has been generally used as a clustering method for investigation of AE features. For example, the characteristics of reduced data vector was adapted to detect damage phases under corrosion attacks (Manson *et al.* 2001). It is worth mentioning that the results of a PCA are highly dependent on the input features. The selection of representative features depends on the type of damage, applied load and type of material (Degala *et al.* 2009).

2.3 K-means clustering

K-means clustering method is a widely used data clustering technique for unsupervised learning tasks (Godin *et al.* 2005, Godin *et al.* 2004). This technique aims at dividing a n -dimension data set \mathbf{X} into k clusters by minimizing a clustering criterion. In this study the adopted clustering criterion is the Euclidean distance (Likas *et al.* 2003), defined as

$$E(m_1, m_2, \dots, m_k) = \sum_{i=1}^N \sum_{j=1}^k I(x_i \in C_j) \|x_i - m_j\|^2 \quad (3)$$

In Eq. (3) m_j is the centroid of j -th cluster, C_j ; and $I(Y)$ is equal to 1 if Y is true and 0 otherwise. The minimization of the criterion is an iterative procedure, consisting of the following steps.

1. Definition of arbitrary centroids of the k clusters.
2. Identification of the cluster for each data x_i in the input vector, in such a way that the data belongs to the cluster with the closest centroid (minimum value of the Euclidean distance).
3. The centroids for k clusters are evaluated again as the mean of the cluster data.
4. The procedure is repeated until the change in the clusters centroids is less than a certain threshold.

The main disadvantage of the k -means algorithm is that the number of clusters, k , is not known a priori. Many criteria have been developed and in this study the proper value k of clusters is defined by means of the Davies-Bouldin (D-B) index (Davies and Bouldin 1979). This index is defined as

$$DB = \frac{1}{k} \cdot \sum_{i=1}^k \max \left\{ \frac{e_h + e_i}{d_{ih}} \right\} \quad (4)$$

in which k is the number of the cluster, e_i and e_h are the distances between the data and the centroids of the classes i and h and d_{ih} is the distance between the centroids that identify clusters i and cluster h . According to the definition, the best index is the smallest one, since it correspond to clusters that are compact, and far from each other.

In this paper, K -means clustering method allows a more rational study of PCA results. The adopted principal components should describe the damage stages and the K -means clustering method can allow individuating the different stages by defining different clusters of data.

3. Experiments

An accelerated corrosion test was carried out on a prestressed seven-wires strand (Fig. 2). Table 2 summarizes the main properties of the tested strand. The test aimed at describing the behavior of a prestressed cable during its lifetime, i.e., under corrosion attack and under very large tensile loadings.

A loading apparatus was designed in order to corrode the strand under axial tensile load. The apparatus consists of two I-shape rigid beams (web: 76.2 cm×7.6 cm×1.9 cm, flanges: 50.8 cm×1.3 cm), located at the opposite sides of the tank and connected by two 28 mm all-thread steel bars. The strand passes through the middle of the I-beams and is tightened by the nuts and the anchorage, as shown in Fig. 3. The initial load applied to the strand was 89 kN (20 kips), while the actual load, recorded before the accelerated corrosion test, was 83 kN (18 kips). These load losses were mostly caused by the steel relaxation.

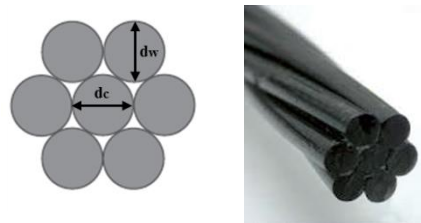


Fig. 2 Seven-wires steel strand

Table 2 Main characteristics of the steel strand

Helicoidal wire diameter (d_w)	[mm (inches)]	5 (1.97)
Core wire diameter (d_c)	[mm (inches)]	5.2 (2.05)
Young modulus E	[GPa]	196
Poisson' ratio	[-]	0.29
Yielding load	[kN]	203
Ultimate tensile strength	[MPa]	1860
Linear weight	[kg/m]	1.10

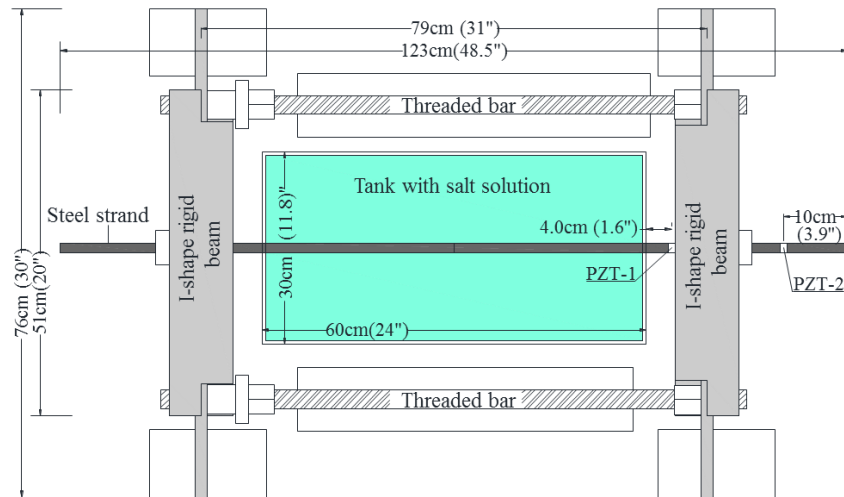


Fig. 3 The loading apparatus for the corrosion test (Farhidzadeh and Salamone 2014)

The accelerated corrosion test was performed by immersing the strand in a 3.5% sodium chloride solution (NaCl), and impressing a direct current by a power supply (Austin *et al.* 2004), as shown in Fig. 4 (Farhidzadeh and Salamone 2014). The test consisted of 13 steps that lasted 25 days (see Table 3). For each step the following protocol was performed: 1) immersion of the specimen in the salt solution; 2) applying voltage; 3) washing with tap water, drying and cleaning the specimen. The applied voltage was 0.16 V until the 11th step and doubled to 0.32 V until the test end. The deriving current started from 0.5 A and increased to about 1.5 A after doubling the potential. The three times higher value after the doubled voltage is justified by the decreased resistance due to the presence of the corroded particles in the salt water. The test was interrupted when three helicoidal wires failed. The core wire remained pristine.

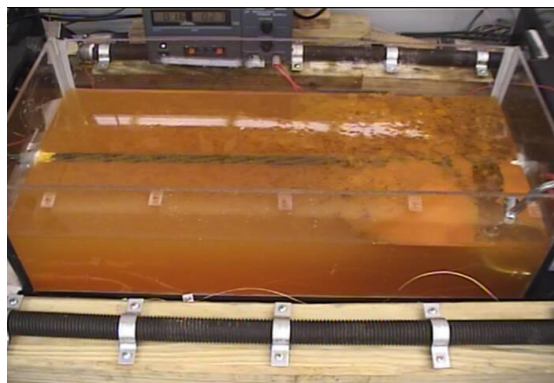


Fig. 4 Corrosion test with impressed current technique on a single steel strand in a salt solution (Farhidzadeh 2014)

Table 3 Testing time of the steps

Step	Start day	End day
1	Oct 3 rd	Oct. 4 th
2	Oct. 4 th	Oct. 6 th
3	Oct. 6 th	Oct. 7 th
4	Oct. 7 th	Oct. 8 th
5	Oct. 8 th	Oct. 9 th
6	Oct. 9 th	Oct. 10 th
7	Oct. 10 th	Oct. 11 th
8	Oct. 11 th	Oct. 14 th
9	Oct. 14 th	Oct. 16 th
10	Oct. 16 th	Oct. 18 th
11	Oct. 18 th	Oct. 21 th
12	Oct. 22 nd	Oct. 24 th
13	Oct. 25 th	Oct. 27 th



Fig. 5 Installed PZT transducers (Farhidzadeh 2014)

The strand was instrumented with two permanently attached PZT (Lead Zirconate Titanate) transducers to receive AE signals. The PZTs were attached on one of the helicoidal wires using epoxy glue along the length of the strand, as shown in Fig. 5. Specifically, one PZT (PZT-1) was installed close to the immersed part of the steel strand while the second one (PZT-2) was placed far from the tank, as shown in Fig. 3. Acoustic emissions data were recorded with an eight-channels data acquisition system (Physical Acoustic Corporation 2005), and a dedicated software for signal processing and storage (AEwin). Preamplifiers were set to 40 dB gain.

4. Results

During the test the corrosion damage on the strand was visually monitored. Fig. 6 shows the corrosion progression which includes an initial deterioration of the protective layer, a severe

cross-section reduction, and eventually the failure of three helicoidal wires (marked by white arrows). The failure of the wires was caused by the severe corrosion, which induced a loss of cross section of the wires. It is worth mentioning that, negligible damage was observed on the central wire. Fig. 7 shows the tensile load versus the time, expressed in terms of the experimental steps. The decrease of load was slow up to the 12th step, wherein a drop to the value of 68 kN (15.29 kips) was recorded; at the end of the 12th step the load decreased to 54.2 kN (12.18 kips). The first wire broke in the last testing step and the 2nd and 3rd wires simultaneously failed a few minutes later. Both the failures corresponded to two sudden drops in the load curve: 1) from 54.2kN (12.18 kips) to 46.2 kN (10.39 kips) and 2) from 44.8kN (10.07 kips) to 26.4kN (5.93 kips). The second load drop was almost twice the first one, demonstrating that each wire sustained almost equal load values.

Before analyzing the AE data, a filtering process was performed in order to remove the possible noise contained in the raw data. In particular, all the AE data corresponding to some manual operations (i.e., drying and cleaning actions) on the specimen were removed. Other data were also removed since they had some peculiar features; e.g., they were isolated data with very large amplitude values, which do not correspond to any large variations in the load; or significant oscillations in the load values were recorded at those time instants. The initial filtering also removes: i) all the data with very low amplitude, i.e., very close (5%) to the mean threshold, and ii) data points with amplitudes smaller than the threshold.

Moreover, the modified Swansong II filtering procedure (Association of American Railroads 1999, ElBatanouny *et al.* 2014a) was applied (Table 4).

One of the most common ways to infer damage conditions by using AE is by using cumulative plots of some features (see Table 1). In general, the onset of damage, such as cracking, corrosion, and failures, may be identified by sudden changes in the rate of these plots (Di Benedetti *et al.* 2013, Farhidzadeh *et al.* 2013a).

Fig. 8 shows the cumulative RMS distribution versus time for PZT-1 and PZT-2. A number of sudden changes were observed on these curves. For instance, concerning the PZT-1 (black solid line in Fig. 8), two significant changes were observed between the 9th and 10th steps, along with a smaller one at the end of the test. By comparing these results with the damage progression shown in Fig. 6, it can be observed that the cumulative RMS cannot follow the damage deterioration in the strand. Therefore, if the monitoring system would be based on the reading of such a plot, some false alarms could occur. The same conclusion can be drawn by the PZT-2 data (gray solid line in Fig. 8).

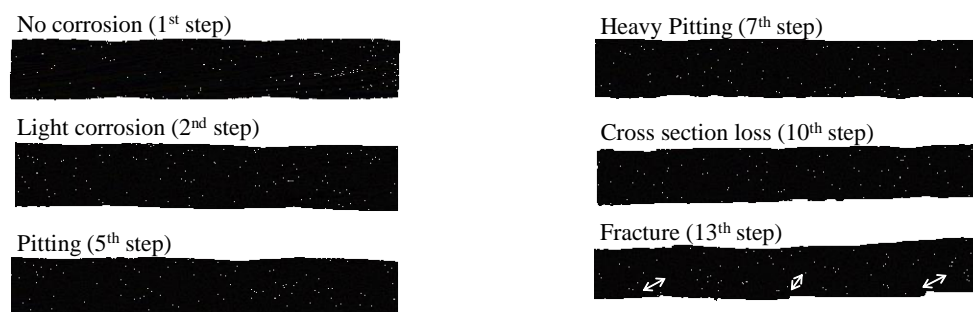


Fig. 6 Corrosion damage stages in the steel strand (Farhidzadeh and Salamone 2014)

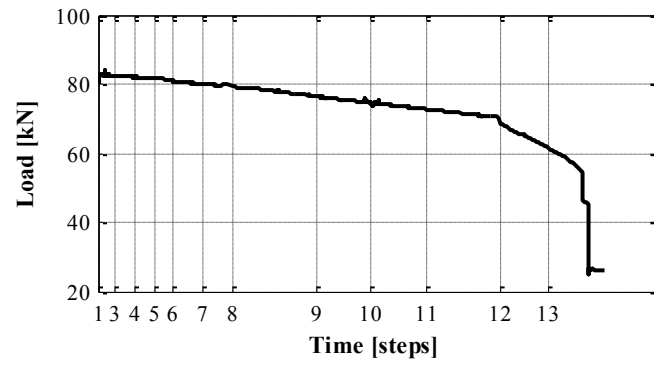


Fig. 7 Load curve during the performed accelerated corrosion test (Farhidzadeh and Salamone 2014)

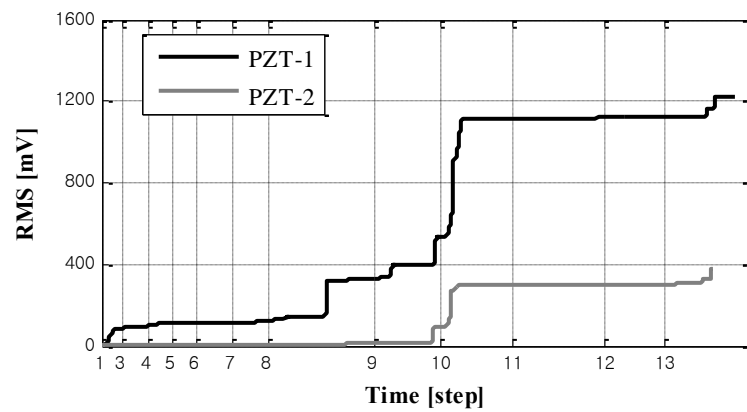


Fig. 8 Cumulative RMS (blue solid curve) versus time (steps) during the corrosion test for PZT-1 (gray solid line) and PZT-2 (black solid line)

Table 4 Adopted modified Swansong II filtering

Amplitude	Duration
[dB]	[usec]
< 60	-
60-67	> 2000
68-75	> 4000
76-83	> 6000
84-91	> 8000
92-100	> 10000

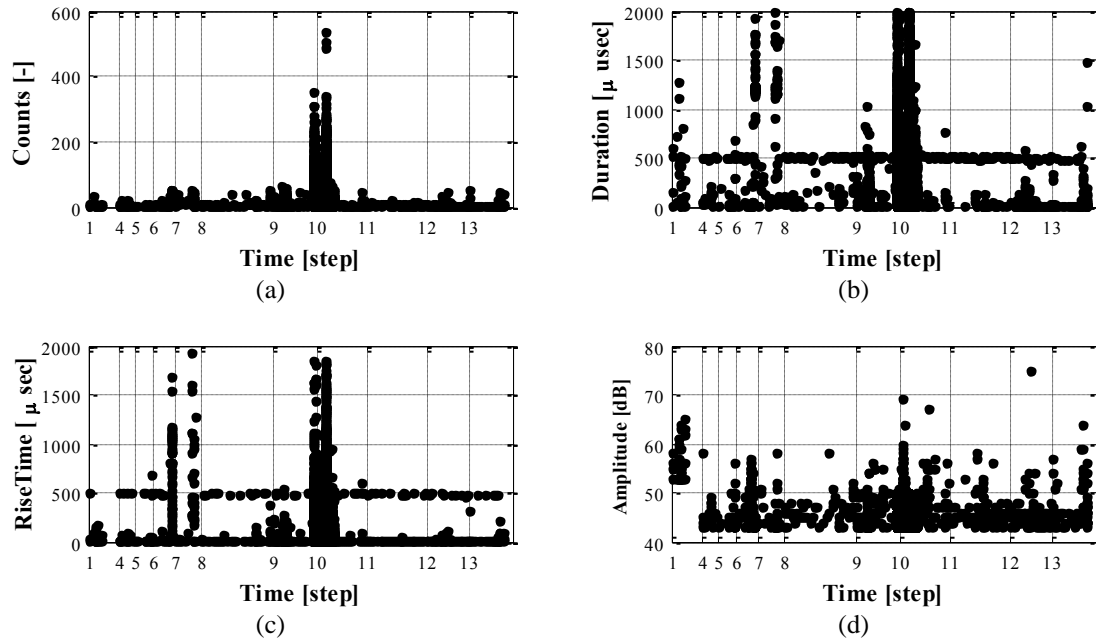


Fig. 9 AE features for PZT-1: (a) counts, (b) duration, (c) rise time and (d) peak amplitude

Fig. 9 shows some AE features, including, rise time, duration, peak amplitude and counts for PZT-1. It can be seen that, a significant AE activity was also recorded in correspondence of steps 9th and 10th, which can be considered as false alarms (no significant damage was observed by visual inspection).

4.1 PCA application

In order to select a set of AE features capable to identify changes in the strand health (e.g., wire failures), and reduce the number of false alarms, a PCA was applied. The AE features used to populate the vector \mathbf{X} defined in Eq. (1), included: rise time, amplitude, duration, counts, RMS, energy, absolute energy (AbE), and RA-value. It should be mentioned that, all the features were normalized before the PCA because of their heterogeneous dimensions. A parametric study was carried out to identify a set of AE features capable to discriminate damage conditions (e.g., wire breakages) from the undamaged state. Fig. 10(a) shows the results of the PCA for the PZT-1 using three features as input variables, that is, amplitude, rise time and duration. Fig. 11 depicts the results of PCA when two more features (i.e., energy and counts) were added into the input vector \mathbf{X} . These results are plotted in terms of the first two principal components because the sum of the variances of these two components (e.g., Fig. 10(b)) is quite large (>78%) and, hence, they are considered reasonably representative of the total variance of the data set. It can be observed that, the selected features do not allow distinguishing different data clusters. Similar results were obtained for PZT-2; however these results were not reported here for the sake of brevity.

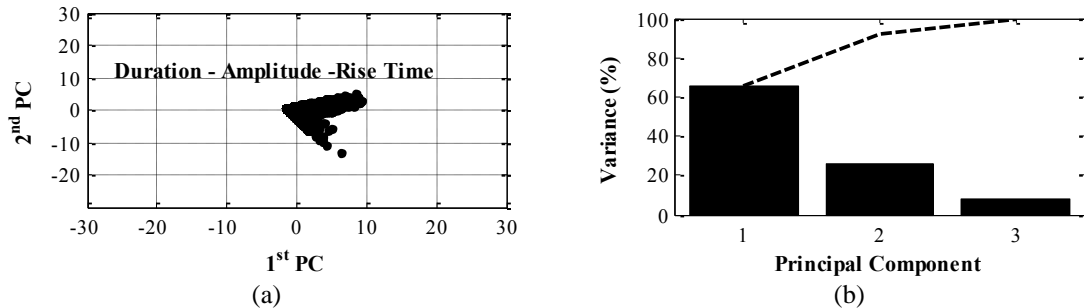


Fig. 10 (a) PCA results for PZT-1 in the first two PCs plane. (b) PC variances (histogram) and sum of the variances (black dash line)

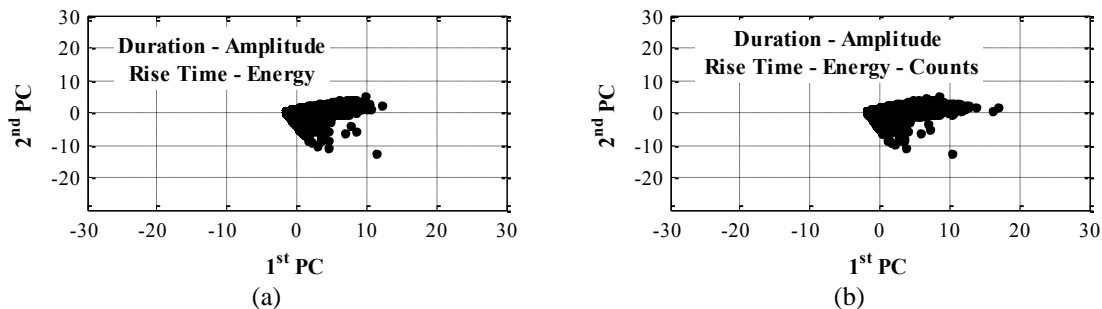


Fig. 11 PCA results for PZT-1 in the first two PCs plane

Fig. 12 shows the PCA results for PZT-1, using RMS, absolute energy (AbE), and RA-value, as input variables. Fig. 13 shows the results for the PZT-2. It can be observed that this set of features can clearly identify two distinct clusters (see Figs. 12(a) and 13(a)). In order to investigate the properties of these two clusters, the data within the Cluster 2 (red circle markers) were superimposed on the load curve (Fig. 7), as shown in Figs. 12(b) and 13(b). Interestingly, these data corresponded to AE signals recorded during the last step, that is, they were generated from the wires failure (load drops). The points of the Cluster 1 belong to all the other time instants of the experimental test; they cannot be correlated to any specific damage change in the strand. Furthermore, it was observed that the points of the Cluster 1 with the larger value of the 1st component (>20), were associated to the unwanted noisy AE data (false alarms); i.e. they belong to the hits in both the 9th and the 10th steps with the abrupt changes in the RMS values. According to this first evidence, the PCA allows identifying the failure moment of the wires from all the other data; on the contrary, the method does not allow identifying other damage levels during the strand deterioration. However, the layout of the no-failure data (values of the points in the Cluster 1) can be used to discriminate the noise in the raw data.

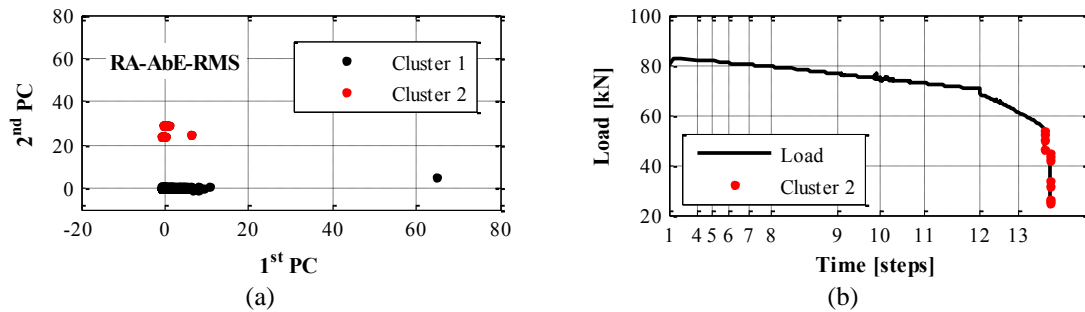


Fig. 12 (a) PCA results for PZT-1 with RMS, absolute energy (AbE) and RA as input variables and (b) identification of the Cluster 2 (red circle markers) on the load curve (black solid line)

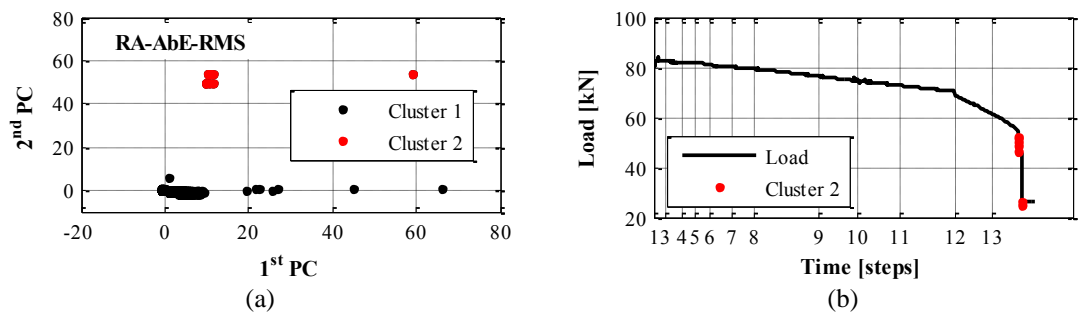


Fig. 13 (a) PCA results for PZT-2 with RMS, absolute energy (AbE) and RA as input variables and (b) identification of the Cluster 2 (red circle markers) on the load curve (black solid line)

4.2 K-means method

Figs. 14(a), and 15(a) show the results of the k-means method applied to the first two principal components, for the PZT-1 and PZT-2. Three input parameters were used, that is, RMS, absolute energy and RA value. As expected, according to the D-B index (Eq. (4)) the best fit clusters number was equal to 3 (see Figs. 14(b) and 15(b)). Three clusters can be identified: 1) Cluster 1, that contains values distributed along the whole corrosion test (black circle markers); 2) Cluster 2, which mostly include data associated to the false alarms (noisy data, gray diamond markers); and 3) Cluster 3 which corresponds to data generated to the wires breakages (red triangle markers).

In this last part of the section, some cluster features are investigated in order to propose an automatic method for the characterization of the data in the identified clusters (i.e., noise or failure). The studied features are: the distance between the clusters centroids (cluster distance) and the distance between the points in a cluster and its centroid (error), evaluated according to Eq. (3).

Fig. 16 shows the distance between the clusters centroids (cluster distance) and the distance between the points in a cluster and its centroid (error), evaluated according to Eq. (3), for PZT-1 and PZT-2. The histograms heights represent the distance of the *i*-th cluster from the other two clusters (*j*-th clusters), then the error is plotted as a function of the number of clusters. The failure cluster (Cluster 3) had the smallest error value and the biggest centroids distances. On the contrary, Cluster 2 shown small values of distance from the “no-damage” cluster (Cluster 1) and it had the largest errors for both the PZTs.

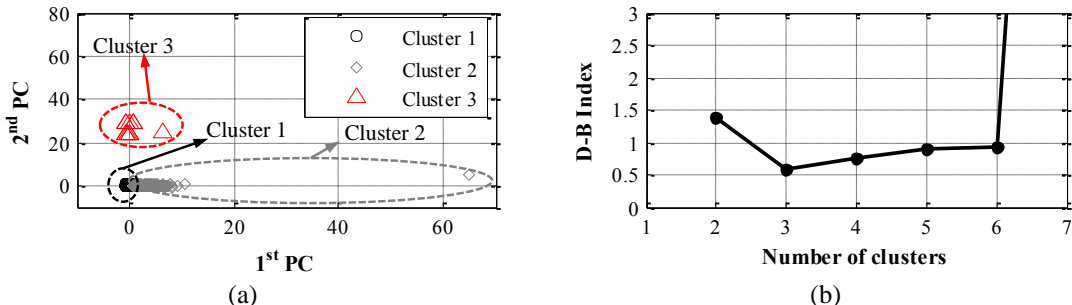


Fig. 14 (a) PCA results for PZT-1 and clusters identification by means of the k-means method. The input parameters are: absolute energy, RMS and RA and (b) Davies-Bouldin index

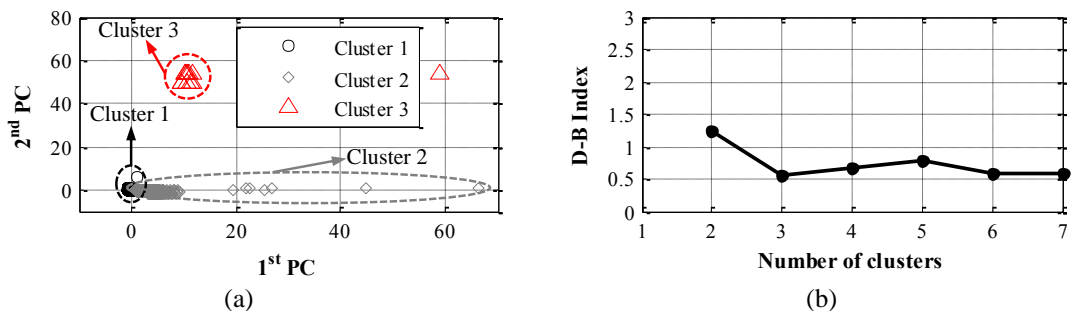


Fig. 15 (a) PCA results for PZT-2 and clusters identification by means of the k-means method. The input parameters are: absolute energy, RMS and RA and (b) Davies-Bouldin index

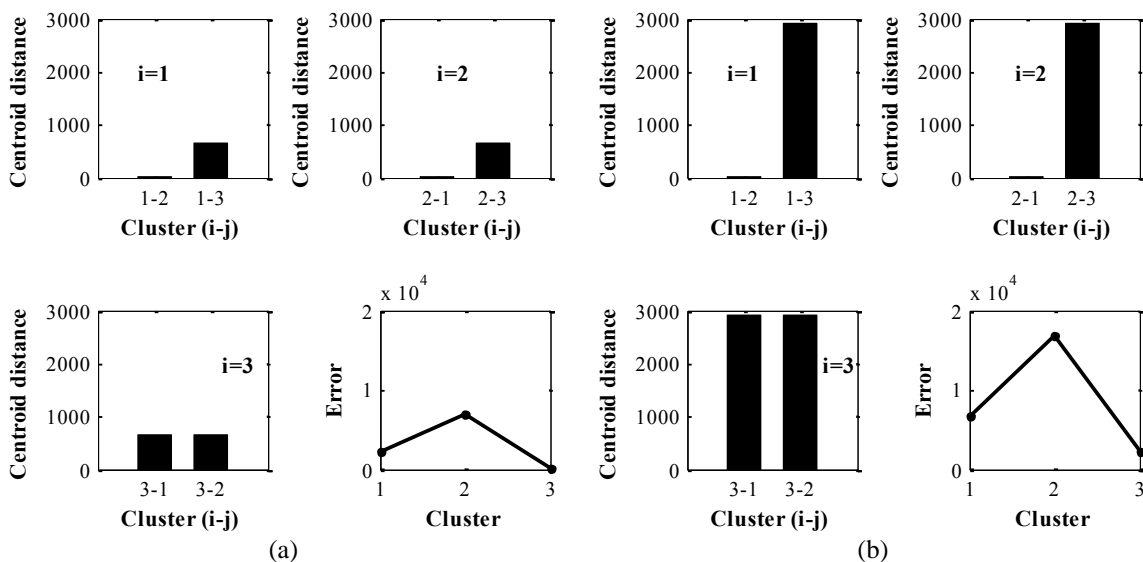


Fig. 16 Centroid distances of the i-th cluster from the j-th clusters (histograms) and cluster errors (black line) for (a) PZT-1 and (b) PZT-2.

These evidences show that the study of the AE with the PCA and the k-means method could be also an efficient way to distinct the failure/damage cluster from the noise data during the monitoring of the element. Hence, during the AE monitoring the identified clusters could be analyzed in terms of both errors and cluster distances: if both the centroid distances of a cluster are larger than distance threshold and its error is lower than an error threshold, the procedure identifies the failure/damage achievement in the element and a health alarm occurs. It is worth to note that the described results are referred to the filtered AE records: some noise data have already been removed from the raw data in a preliminary phase (see Section 3.1). However, the proposed approach is still valid since the adopted filter (Swansong) can also be used during the real monitoring of structural elements. The approach should allow the identification of the other likely noise data, which cannot be easily removed and recognized by standard filtering methods. However, additional tests need to be conducted to verify the robustness of the proposed approach, for instance by means of non-accelerated corrosion test.

5. Conclusions

This paper presented the results of an accelerated corrosion test on a seven-wire steel strand under a constant tensile force. The strand was instrumented with two permanently attached PZT transducers to receive AE signals. The PZTs were attached on one of the helicoidal wires using epoxy glue along the length of the strand. The strand experienced significant corrosion damage, that is cross-section loss and eventually wire breakages. A preliminary study on traditional AE features was performed, and it was observed that although these features were able to identify the failure of the strand, a number of false alarms were triggered. In order to find a more reliable and efficient way to correlate the AE data to the corrosion damage, and reduce the number of false alarms, the k-means method was applied via PCA of AE features. It was shown that the capability of the PCA method is highly affected by the input variables. If time-driven parameters (Absolute energy or RMS) and low-noise sensitive features (RA values) are used, the method gives a very good correlation between the failure and the AE clusters. On the contrary, if very noise sensitive parameters (e.g., counts, rise time) are used, the PCA does not allow defining any correlation between the data and the damage in the material. Moreover, this study shows that the noise data could be identified by studying some features of the clusters, defined by the PCA and the k-means method. However, additional tests need to be conducted in order to verify the robustness of the proposed approach, for instance by means of non-accelerated corrosion test.

Acknowledgments

The financial support for this study was provided in part by the Research Foundation for the State University of New York, through the Research Collaboration Fund, and the Research and Innovative Technology Administration of the U.S. Department of Transportation through the University Transportation Centers program.

References

- Andrade, C., Alonso, C., Gulikers, J., Polder, R., Cigna, R., Vennesland, O., Salta, M., Raharinaivo, A. and Elsener, B. (2004), "Test methods for on-site corrosion rate measurement of steel reinforcement in concrete by means of the polarization resistance method", *Mater Struct.*, **37**(273), 623-643. Doi 10.1007/Bf02483292
- Association of American Railroads (1999), *Procedure for Acoustic Emission Evaluation of Tank Cars and IM-101 Tanks*, (Issue 8. Operation and Maintenance Department), Washington DC.
- ASTM (2009), *Standard test method for half-cell potentials of uncoated reinforcing steel in concrete*, West Conshohocken.
- Austin, S.A., Lyons, R. and Ing, M.J. (2004), "Electrochemical behavior of steel-reinforced concrete during accelerated corrosion testing", *Corrosion*, **60**(2), 203-212.
- Bartoli, I., Phillips, R., di Scalea, F.L., Salamone, S., Coccia, S. and Sikorsky, C.S. (2008), "Load monitoring in multiwire strands by interwire ultrasonic measurements", *Proc Spie*, **6932**. Artn 693209 Doi 10.1117/12.775934
- Beard, M.D., Lowe, M.J.S. and Cawley, P. (2003), "Ultrasonic guided waves for inspection of grouted tendons and bolts", *J. Mater. Civil Eng.*, **15**(3), 212-218. Doi 10.1061/(Asce)0899-1561(2003)15:3(212)
- Behnia, A., Chai, H.K. and Shiotani, T. (2014), "Advanced structural health monitoring of concrete structures with the aid of acoustic emission", *Constr Build Mater*, **65** 282-302. <http://dx.doi.org/10.1016/j.conbuildmat.2014.04.103>
- Choi, O., Park, Y. and H., R. (2008), *Corrosion Evaluation of Epoxy-coated Bars by Electrochemical Impedance Spectroscopy*, International Concrete Abstracts Portal.
- Davies, D.L. and Bouldin, D.W. (1979), "Cluster Separation Measure", *IEEE T. Pattern Anal.*, **1**(2), 224-227.
- Degala, S., Rizzo, P., Ramanathan, K. and Harries, K.A. (2009), "Acoustic emission monitoring of CFRP reinforced concrete slabs", *Constr. Build. Mater.*, **23**(5), 2016-2026. DOI 10.1016/j.conbuildmat.2008.08.026
- Di Benedetti, M., Loreto, G., Matta, F. and Nanni, A. (2013), "Acoustic Emission Monitoring of Reinforced Concrete under Accelerated Corrosion", *J. Mater. Civil. Eng.*, **25**(8), 1022-1029. Doi 10.1061/(ASCE)MT.1943-5533.0000647
- ElBatanouny, M.K., Larosche, A., Mazzoleni, P., Ziehl, P.H., Matta, F. and Zappa, E. (2014a), "Identification of cracking mechanisms in scaled FRP reinforced concrete beams using acoustic emission", *Exp Mech*, **54**(1), 69-82. DOI 10.1007/s11340-012-9692-3
- ElBatanouny, M.K., Mangual, J., Ziehl, P.H. and Matta, F. (2014b), "Early corrosion detection in prestressed concrete girders using acoustic emission", *J. Mater. Civil Eng.* **26**(3), 504-511. doi:10.1061/(ASCE)MT.1943-5533.0000845
- Elfergani, H.A., Pullin, R. and Holford, K.M. (2013), "Damage assessment of corrosion in prestressed concrete by acoustic emission", *Constr. Build. Mater.*, **40** 925-933. <http://dx.doi.org/10.1016/j.conbuildmat.2012.11.071>
- Elsener, B., Andrade, C., Gulikers, J., Polder, R. and Raupach, M. (2003), "Half-cell potential measurements - Potential mapping on reinforced concrete structures", *Mater Struct*, **36**(261), 461-471. Doi 10.1007/Bf02481526
- Ervin, B.L., Kuchma, D.A., Bernhard, J.T. and Reis, H. (2009), "Monitoring corrosion of rebar embedded in mortar using high-frequency guided ultrasonic waves", *J. Eng. Mech.- ASCE*, **135**(1), 9-19. Doi 10.1061/(ASCE)0733-9399(2009)135:1(9)
- Farhidzadeh, A. (2014), *Application of Pattern Recognition Algorithms and Nondestructive Evaluation Techniques for the Structural Health Monitoring of Civil Structures*, PhD dissertation, Department of Civil, Structural, and Environmental Engineering, University at Buffalo, Buffalo, NY, USA.
- Farhidzadeh, A. and Salamone, S. (2014), "Reference-free Corrosion Damage Diagnosis in Steel Strands Using Guided Ultrasonic Waves (under review)", *Ultrasonics*.

- Farhidzadeh, A., Salamone, S., Luna, B. and Whittaker, A. (2013a), "Acoustic emission monitoring of a reinforced concrete shear wall by b-value-based outlier analysis", *Struct. Health Monit.*, **12**(1), 3-13. Doi 10.1177/1475921712461162
- Farhidzadeh, A., Salamone, S. and Singla, P. (2013b), "A probabilistic approach for damage identification and crack mode classification in reinforced concrete structures", *J. Intell. Mat. Syst. Str.*, **24**(14), 1722-1735. Doi 10.1177/1045389x13484101
- Godin, N., Huguet, S. and Gaertner, R. (2005), "Integration of the Kohonen's self-organising map and k-means algorithm for the segmentation of the AE data collected during tensile tests on cross-ply composites", *NDT&E Int.*, **38**(4), 299-309. DOI 10.1016/j.ndteint.2004.09.006
- Godin, N., Huguet, S., Gaertner, R. and Salmon, L. (2004), "Clustering of acoustic emission signals collected during tensile tests on unidirectional glass/polyester composite using supervised and unsupervised classifiers", *NDT & E Int.*, **37**(4), 253-264. DOI 10.1016/j.ndteint.2003.09.010
- Li, Z.J., Li, F.M., Zdunek, A., Landis, E. and Shah, S.P. (1998), "Application of acoustic emission technique to detection of reinforcing steel corrosion in concrete", *ACI Mater. J.*, **95**(1), 68-76.
- Likas, A., Vlassis, N. and Verbeek, J.J. (2003), "The global k-means clustering algorithm", *Pattern Recogn.*, **36**(2), 451-461. [http://dx.doi.org/10.1016/S0031-3203\(02\)00060-2](http://dx.doi.org/10.1016/S0031-3203(02)00060-2)
- Mangual, J., ElBatanouny, M., Ziehl, P. and Matta, F. (2013), "Corrosion damage quantification of prestressing strands using acoustic emission", *J. Mater. Civil Eng.*, **25**(9), 1326-1334. Doi 10.1061/(ASCE)MT.1943-5533.0000669
- Manson, G., Worden, K., Holford, K. and Pullin, R. (2001), "Visualisation and dimension reduction of acoustic emission data for damage detection", *J. Intell. Mat. Syst. Str.*, **12**(8), 529-536. Doi 10.1106/Ud41-Upgc-Wg29-A341
- Mazille, H., Rothea, R. and Tronel, C. (1995), "An Acoustic-Emission Technique for Monitoring Pitting Corrosion of Austenitic Stainless-Steels", *Corros. Sci.*, **37**(9), 1365-1375. Doi 10.1016/0010-938x(95)00036-J
- Moustafa, A., Niri, E.D., Farhidzadeh, A. and Salamone, S. (2014), "Corrosion monitoring of post-tensioned concrete structures using fractal analysis of guided ultrasonic waves", *Struct. Control. Health.*, **21**(3), 438-448. Doi 10.1002/Stc.1586
- Naito, C., Sause, R., Hodgson, I., Pessiki, S. and Macioce, T. (2010), "Forensic examination of a noncomposite adjacent precast prestressed concrete box beam bridge", *J. Bridge Eng.*, **15**(4), 408-418. Doi 10.1061/(ASCE)BE.1943-5592.0000110
- Niri, E.D., Farhidzadeh, A. and Salamone, S. (2013), "Adaptive multisensor data fusion for acoustic emission source localization in noisy environment", *Struct Health Monit.*, **12**(1), 59-77. Doi 10.1177/1475921712462937
- Ohno, K. and Ohtsu, M. (2010), "Crack classification in concrete based on acoustic emission", *Constr. Build. Mater.*, **24**(12), 2339-2346. DOI 10.1016/j.conbuildmat.2010.05.004
- Physical Acoustic Corporation (2005), Princeton Junction
- Physical Acoustics (2009), *Sensor Highway II user's manual*, NJ.
- Salamone, S., Veletzos, M.J., Lanza di Scalea, F. and Restrepo, J.I. (2012), "Detection of initial yield and onset of failure in bonded posttensioned concrete beams", *J. Bridge Eng.*, **17**(6), 966-974. doi:10.1061/(ASCE)BE.1943-5592.0000311